CrystEngComm

Accepted Manuscript

ROYAL SOCIETY OF CHEMISTRY

www.rsc.org/crystengcomm

Cite this: DOI: 10.1039/c0xx00000x

www.rsc.org/xxxxxx

ARTICLE TYPE

Two-dimensional self-assembly of single-crystal, poly-crystal and co-crystal at the liquid/solid interface

Pei Liu, Xinrui Miao*, Zhuomin Li, Bao Zha, Wenli Deng*

Received (in XXX, XXX) Xth XXXXXXXXX 20XX, Accepted Xth XXXXXXXXX 20XX

DOI: 10.1039/b000000x

Studying two-dimensional (2D) and three-dimensional (3D) crystallization in close tandem is a powerful way to acquire a deep understanding of molecular self-assembly. X-ray crystallography results indicate that **C1**, **C2** and **C3** are single-crystal, poly-crystal and co-crystal, respectively. Furthermore, the self-assembled structures of these three kinds of crystals (**C1**–**C3**) at 1-phenyloctane/HOPG interface are observed by scanning tunneling microscopy at ambient conditions. **C1** molecule with a short chain is lying flat on the substrate with a close packing phase, which is the same with its 3D crystal. **C2** molecule bearing a longer chain forms two types of linear structures, which are stable enough to endure continuous tip scanning. In Type I, **C2** molecules lie flat on the substrate to form a zigzag linear pattern, while in Type II one of fluorene cores in each **C2** molecule adopts an edge-on arrangement and interlocks with adjacent fluorene core in one lamella. In co-crystal **C3**, naphthalene-1,5-diamine and 9-fluorenone arrange perpendicular to the HOPG surface in a herringbone pattern by hydrogen bonds and π–π interactions. The lying or standing orientation of three kinds of crystals shows that the middle spacer tethered functional groups can modulate the motifs of self-assemblies in 2D and 3D. Furthermore, it also highlights that physical adsorption on the HOPG surface is not only controlled by the adsorbate-substrate interactions but also by the size and shape of adsorbates.

Introduction

Scanning tunneling microscopy (STM) is a technique which allows the investigation of self-assembled monolayers (SAMs) both at the graphite-solution interface and on dry graphite surface with molecular resolution. It requires two important conditions for the formation of SAMs: the incentive force and the guidance.[1] The incentive force refers to the synergy of all kinds of weak intermolecular interactions, which provide the energy required. And the guidance means the complementarity of structures in the space, that is to say, the spatial size and direction must fulfill the requirements of molecular rearrangement for the molecular self-assembly. Ultimately, the SAMs formation is a dynamic process and essentially depends on the adsorption–desorption equilibrium toward a minimum of the overall free energy.[2-3] In terms of the chemical reaction kinetic, successful STM imaging at the interface is the result of the interplay of adsorbate–adsorbate and adsorbate–substrate interactions. Thus, it is essential to understand and utilize these mutual effects for realization of the desired organic nanostructures with special electronic functions.

The two-dimensional (2D) nanostructures of various kinds of molecules have been investigated by self-assembly technique with STM, such as long-chain alkanes,[4] aromatic compounds,[5] conducting polymers,[6] chiral crystals,[7] nucleotides,[8] dyes,[9] and polypeptides.[10] Particularly, π-conjugated molecules have been of great interest in the field of organic electronics materials because of their eminent electronic and photophysical properties as promising materials.[11-14] In particular, owing to their reasonable light emitting properties, fluorene-based materials were studied extensively during recent years acting as high performance blue emitters for applications in organic light-emitting diodes (OLEDs).[15-18] From a synthetic point of view, fluorene can be connected to other functional groups at the 9-position, yielding a series of derivatives with different groups and chemical functionalities. In addition, fluorene derivatives possessing a binary symmetry confer very excellent properties as they show high fluorescence efficiency in the solid state.[19] Most studies about fluorene derivatives focus on the synthesis or photovoltaic properties.[20] In order to better understand the complex charge transport processes in thin films, a detailed observation of the morphology of the active layer is highly desirable. However, up till now, to our knowledge, there have been few cases on the self-assembly investigation of fluorene derivatives by STM.[21] Furthermore, no results on the self-assembly of co-crystals have been reported yet.

Herein, we report on the self-assembly behaviors of **C1**, **C2** and **C3** on the HOPG surface (Scheme 1). Previous reports have indicated that the crystal forms of **C1** and **C3** were single-crystal and co-crystal, respectively.[22-23] Our X-ray diffraction result shows that the crystal form of **C2** is polycrystalline. These three kinds of crystals can form regular 2D crystallized films at the 1-phenyloctane/HOPG interface, which can be clearly observed by STM. **C1** molecule with a short alkyl chain is observed to produce the ordered molecular assembly structures with flat lying

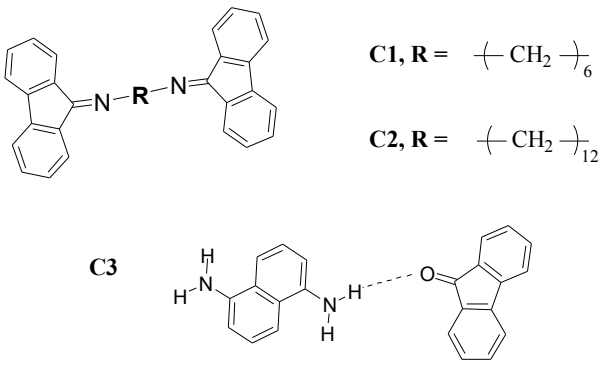

Scheme 1 Chemical structures of 9-fluorenyl Schiff bases derivatives (**C1**, **C2**, and **C3**). **C1**: N-[6- (fluoren-9-ylideneamino)hexyl]fluoren-9-imine; **C2**: N-[12-(fluoren-9-ylideneamino)dodecyl] fluoren-9-imine; **C3**: Co-crystal of naphthalene-1,5-diamine and 9-fluorenone.

configuration by intermolecular hydrogen-bonding interactions, which is the impressive homology with 3D crystal. **C2** molecule with a longer alkyl chain forms two types of linear structures as a joint result of intermolecular interactions and molecular–substrate interactions. We deduce that the self-assembled polymorph of **C2** in 2D is associated with its polycrystalline structure in 3D. Co-crystal (**C3**) of naphthalene-1,5-diamine and 9-fluorenone grow along the crystallographic *b* axis through hydrogen-bonding interactions and π–π stacking in a herringbone fashion, in which the intermolecular interactions dominate the morphology. It is obvious that the assembly patterns of these crystals on graphite surfaces can be deliberately manipulated by the changes of functional group and intermolecular interaction, which is related to their crystal forms in 3D. Our work studying 2D and 3D crystallization in close tandem provides a powerful way to acquire a deep understanding of molecular self-assembly.

Experimental section

X-ray diffraction

The three kinds of crystals were synthesized in our lab.[22] The powder X-ray diffraction (XRD) patterns were carried out by Bruker D8-ADVANCE diffractometer with Cu Kα radiation. A step scan mode was adopted with a sampling time of 0.1 s and a scanning step of 0.02°. The XRD peaks of all samples can be indexed by using Dicvol program.

The STM investigation

All experiments were carried on a Nanoscope Multi-mode IIIa SPM (Bruker, USA) at ambient conditions. Scanning tunneling microscopy (STM) was operated in constant-current mode with the tip mechanically cut from Pt/Ir wires (80/20). 1-Phenyloctane (99+ %) used were purchased from Aldrich. Each investigated compound was dissolved in solvent to form a saturated solution and then a small droplet (~2 μl) of the solution was deposited on the freshly cleaved atomically flat surface of HOPG (quality ZYB, Bruker, USA) for STM observations. In order to allow imaging of the HOPG surface underneath the molecules, the scanner was calibrated in situ by raising the tunneling current to 1 nA and allowing the bias voltage to 100 mV before and after the experiments. All the images were processed only by the application of a background flattening.

Molecular models

Molecular models of the assembled structures were built by Materials Studio 4.4. The model of monolayer was constructed by placing the molecules according to the intermolecular distances and angles that were obtained from the analysis of STM images.

Results and discussion

X-ray diffraction (XRD) was carried out to detect the molecular packing in the 3D solid-state. Our group and Ding et al. have reported that the crystal forms of **C1** and **C3** were single-crystal and co-crystal, respectively, by single-crystal X-ray diffraction.[22-23] The powder X-ray diffraction patterns of compound **C1** and **C2** are presented in Fig. 1. The relatively sharp and intense peaks of **C1** and **C2** suggest that the crystals are highly crystalline and purified. The diffraction peaks of **C1** can be well indexed to monoclinic system with a space group of P2(1)/c, which in good agreement with the literature values. Compound **C2** belongs to monoclinic system, space group P2(1)/c, with a = 9.1029 Å, b = 17.2178 Å, c = 9.9998 Å; β = 107.162°; V = 1497.50 Å^3. The sharp and narrow range of diffraction peaks at 2θ = 10-30° in the sample of **C2** indicate that the products have a typical crystalline state. However, based on our previous studies, the crystal of **C2** molecule is too thin to be characterized by X-ray single-crystal diffraction. So we can infer that the crystal form of compound **C2** is polycrystalline.

In order to compare the difference of molecular packing in two- and three- dimension spaces, we are motivated to investigate the 2D self-assembly behavior of these three kinds of crystals on the HOPG surface. To the best of our knowledge, many studies have focused on the introduction of conjugated groups to increase the conjugacy and thermal stability of fluorene derivatives.[24] And as the increase of molecular conjugation degree, the absorption and emission wavelength is changing along with it. In general, the introduction of flexible carbon chain at 9-position can increase the solubility of fluorene and prevent the occurrence of defects.[25-26] Thus, we first use linear alkyl chain to separate two fluorene cores through 9-position (**C1**–**C2**), and then investigate the influence of different length of alkyl spacer on the adsorbed structures. The conjugation degree of fluorene would not increase in theory due to the alkyl chain, but it is anticipated to adjust the

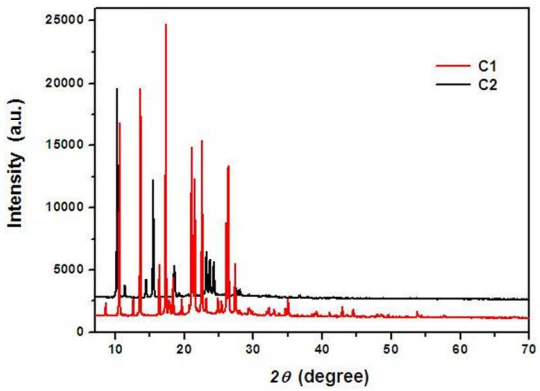

Fig. 1 X-ray diffraction patterns of compound **C1** and **C2**.

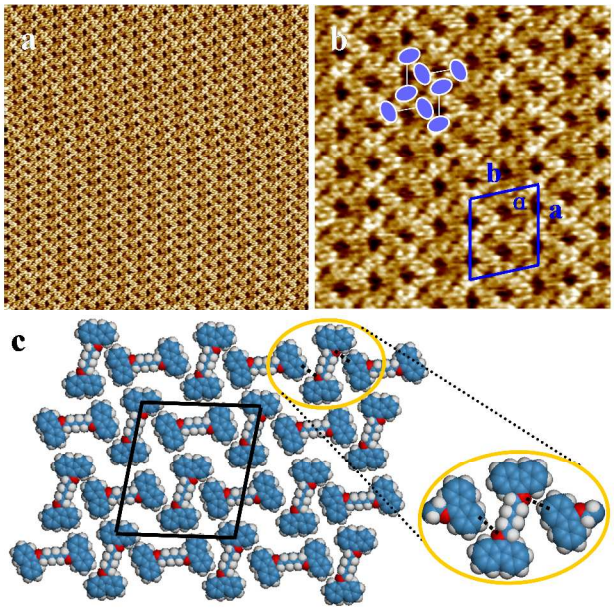

Fig. 2 (a) Large-scale STM image of **C1** self-assembly at 1-phenyloctane/HOPG interface at room temperature. Scan area: 50 nm × 50 nm; Tunneling conditions: V_{bias} = 773 mV, I_t = 465 pA. (b) High-resolution STM image of **C1** showing the grid pattern with local molecular permutations. Scan area: 15 nm × 15 nm; Tunneling conditions: V_{bias} = 796 mV, I_t = 463 pA. The blue ovals represent the fluorene cores and the white lines in the middle stand for indiscernible alkyl chains. Blue parallelogram in the image shows the unit cell. (c) Structural model of the grid pattern. The black dashed lines in yellow ovals indicate the hydrogen bonds.

2D self-assembly structure on the graphite surface.

The representative STM images of **C1** assembled adlayer obtained at 1-phenyloctane/HOPG interface are shown in Fig. 2. The typical domain size can reach 200 × 200 nm² without obvious defects. Dumbbell-like **C1** molecules form a compact grid pattern as illustrated in Fig. 2a. From the high-resolution STM image (Fig. 2b), we can observe that the entire molecule is lying flat on the substrate and two adjacent molecules interlace with each other by a head-to-belly fashion. The middle alkyl chain cannot be resolved, which is attributed to the low electron density of single alkyl chain. As a consequence of this arrangement, many nanometric-size cavities are formed in the middle of the aggregates. Some fluorene cores have higher contrast than the others, which is caused by periodic modulation of the interaction of molecular lattice with the graphite surface. This extremely stable head-to-belly fashion is related to the size and shape of **C1** molecule. The grid structure has a rhombus unit cell with lattice parameters a = 3.4 ± 0.1 nm, b = 4.1 ± 0.1 nm, and α = 80 ± 2°. A structural model based on the STM images for the grid structure is proposed in Fig. 2c.

The formation of self-assemble structures should be related to the combination of various forces at the liquid/HOPG interface in essential. These forces usually include hydrogen bonding, van der Waals force, electrostatic, dipolar interaction. Specifically, the hydrogen bonds always play an important role in building 2D and 3D nanostructures owing to the relatively strong, selective and directional nature.[27-28] For the self-assembled monolayer of **C1**, the major intermolecular force refers to –C-H…N– hydrogen bonds between hydrogen atoms in fluorene rings of horizontal molecules and nitrogen atoms of adjacent vertical molecules. Although the –C-H…N– interactions are weaker than other types of hydrogen bonds, they are important in improving the stability of 2D structures and should not be neglected for this configuration. Furthermore, **C1** crystallizes in 2D and 3D with impressive homology, [22] which confirms that the grid pattern of **C1** is dominated by the intermolecular interactions, while the substrate plays a less important role.

To probe the impact of alkyl chain length on the self-assembled morphology of 9-fluorenyl Schiff bases derivatives, the adsorption of **C2** on the HOPG surface was investigated by STM. After the experiment was repeated for a few times at 1-phenyloctane/HOPG interface, two types of linear structures can be ascertained. Fig. 3a and 3b present the large-scale STM images of two linear patterns, named as Type I and Type II, respectively. The domain size with regular molecular stripes both extends to 100 nm. Type I features the close-packed zigzag linear structure without well-resolved alkyl chains. While the most-notable peculiarity of Type II is that, the bright lines have a bigger width and higher contrast than Type I and the alkyl chains can be recognized easily.

The structural details of Type I are revealed by a high-resolution STM image as shown in Fig. 3c. The image is sub-molecularly resolved, which enables us to identify the individual molecules as well as their actual arrangement. The fluorene moieties can be discerned evidently as paired leaves of bright spots separated by the dodecyl chains with dark contrast. These bright spots are measured to be 0.9 ± 0.1 nm, which is in agreement with the length of fluorene core calculated by Materials Studio. The average length of adjacent bright spots in neighbor lamellae as the red unit indicated in Fig. 3c is 2.7 ± 0.1 nm, which is consistent with the length of **C2** molecule. The results indicate that the aromatic units are all lying flat on the substrate and the alkyl chains adapt a straight linear configuration. Like the self-assembly of **C1**, the alkyl chains of **C2** in Fig. 3c are hard to be identified because of their large dispersity and low electron density.

On the basis of the STM observation, a structural model for the close-packed Type I linear structure is proposed in the local region of Fig. 3c. A unit cell with a = 3.4 ± 0.1 nm, b = 1.5 ± 0.1 nm, and α = 85 ± 2° is superimposed on the image. The formation of Type I assembly must be originated from the molecule-substrate interaction as well as intermolecular interaction. The former means the van der Waals interaction between molecules and graphite, while the latter mainly refers to the dipole–dipole interaction. Close inspection of the image reveals that the two neighboring stripes are actually different. From the schematic drawing in Fig. 3e, it can be seen that the **C2** molecules alternatively take a reverse orientation in adjacent molecular rows. A schematic of dipolar alignments of Type I structure is shown in Fig. 3e. From the perspective of a single molecule, the dipoles on both ends of the molecule would align antiparallelly, as shown on the top of Fig. 3e. While when forming the 2D linear structure, the fluorene cores in different molecules in the same lamellae can form dipole pairs more easily, because they get closer than the two end groups of single molecule. The dislocated arrangement of Schiff base dipoles can separate neighboring molecular dipole pairs to avoid the potential dipole repulsion. [29] It

can be evidently

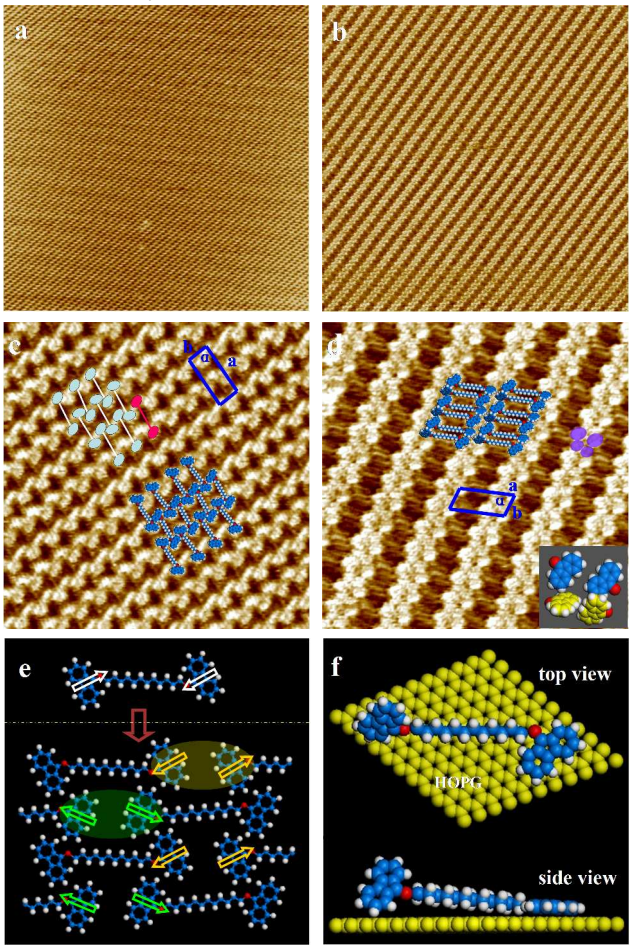

Fig. 3 Large-scale (a) and high-resolution (c) STM images showing **C2** physisorbed monolayer (Type I) at 1-phenyloctane/HOPG interface. (a) 100 nm × 100 nm, V_{bias} = 785 mV, I_t = 467 pA. (c) 20 nm × 20 nm, V_{bias} = 796 mV, I_t = 459 pA. Large-scale (b) and high-resolution (d) STM images of **C2** self-assembled monolayer (Type II). (b) 100 nm × 100 nm, V_{bias} = 812 mV, I_t = 451 pA. (d) 20 nm × 20 nm, V_{bias} = 794 mV, I_t = 468 pA. (e) Schematic diagram with dipole alignments for Type I. (f) Side view and top view models of individual edge-on molecule in Type II.

seen that, the dipole–dipole interaction of Schiff bases plays a leading role in determination of the Type I structure.

Fig. 3d presents a high-resolution STM image acquired for Type II structure of **C2** monolayer on the HOPG surface. The conjugated moieties are generally identified as bright contrast protrusions since they have a larger electronic coupling with the STM tip than the methylene groups. So the bright stripes can be ascribed to the fluorene units of **C2** molecules whereas the dark troughs correspond to alkyl chains. As resolved from the image, the aromatic rings in the bright strips form a close-packed pattern separated by the alkyl chains. Every four bright spots form a tetramer that consists of two dimers as the purple ovals shown in Fig. 3d. Two fluorene cores in the tetramer are measured to be 0.9 ± 0.1 nm, indicating they are lying flat to the substrate. The remaining pair is measured to be 0.6 ± 0.1 nm, much shorter than the theoretically calculated length, suggesting that the conjugated moieties are tilted from the HOPG surface and adopt an edge-on arrangement. This is because of the free torsion around the –C=N– bond that connects fluorene unit and alkyl chain. The angle of the tilted plane β can be calculated from cosβ = 0.6/0.9 to be 42°. A tentative model of **C2** on the graphite surface is given in Fig. 3d. Neighboring molecules in the same lamella are rotated by 180° with respect to each other. The parameters of unit cell are measured to be a = 3.5 ± 0.1 nm, b = 1.5 ± 0.1 nm, and α = 72 ± 2°. It is worth noting that the tilted fluorene pairs may partially interlocked with each other since they stay too close (Fig. 3f). The root cause is the hydrogen atoms of neighbouring fluorenes on the contact region mesh due to steric hindrance. This complementary action between the binding aromatic units bestows to this linear structure a strong orientational stability. [30] In addition, the tilted fluorene core has an edge-to-face interaction with the face of the neighboring aromatic ring owing to the face-tilted T-geometry. The edge-to-face interaction can be seen as an unconventional hydrogen bonding, namely –C-H…π-interaction.[31-32] Generally, the most optimum orientations adopted by the molecules on the graphite substrate tend to minimize the surface stress. In this ordered stripe-like structures, alkyl chains arrange along preferential substrate directions resulting in the breakdown of anisotropy of the surface stress, and in turn limits the flat adsorption of fluorene units. This edge-on configuration decrease the van der Waals interactions between molecule and graphite lattice but greatly increase the interactions among fluorene units, making the self-assembly monolayer effectively stabilized.

Average area per molecule and free energy can be used to compare the stability of lamellar structures on the surface.[33] According to the crystal lattice parameters, the average area per molecule is 2.54 ± 0.02 nm2 in Type I and 2.50 ± 0.02 nm2 in Type II. The close value demonstrates that the two patterns have the same stability on the graphite surface. In fact, these two types of linear structures could coexist (Fig. S1, ESI) and were stable enough to go through continuous tip scanning, respectively. However, due to the rapid structural transformation and the high mobility of C2 molecules during scanning, it is not easy to obtain high-resolution mixed nanopattern images. From the point of view of thermodynamics, the observation of coexistence of both polymorphs within the same concentration under ambient conditions can be taken as an indication that their free energies are very similar. As mentioned above, the crystal of **C2** molecule is too thin to be characterized by X-ray single-crystal diffraction. In addition, XRD result indicates that **C2** is polycrystalline. So it is not easy to get the large-scale stacking pattern of **C2** in 3D. The different configurations appeared in the self-assembly also reveal the fact that **C2** molecules cannot form single crystals because of the increase of molecular flexibility.

According to the results of single crystal X-ray diffraction of co-crystal **C3**, [23] the naphthalene-1,5-diamine molecules are staggered parallel with each other along the c-axis, while fluorenone units are anti-parallel along the c-axis as well. The weak π–π interactions lead to these column π-stacking configurations due to the π-extensional electronic structure of aromatic moieties. Additionally, naphthalene-1,5-diamine and 9-fluorenone contact each other through a strong –N-H…O– hydrogen bonding. So one naphthalene-1,5-diamine molecule can form hydrogen bonds with four fluorenone molecules, while one fluorenone molecule can form hydrogen bonds with two naphthalene-1,5-diamine molecules.

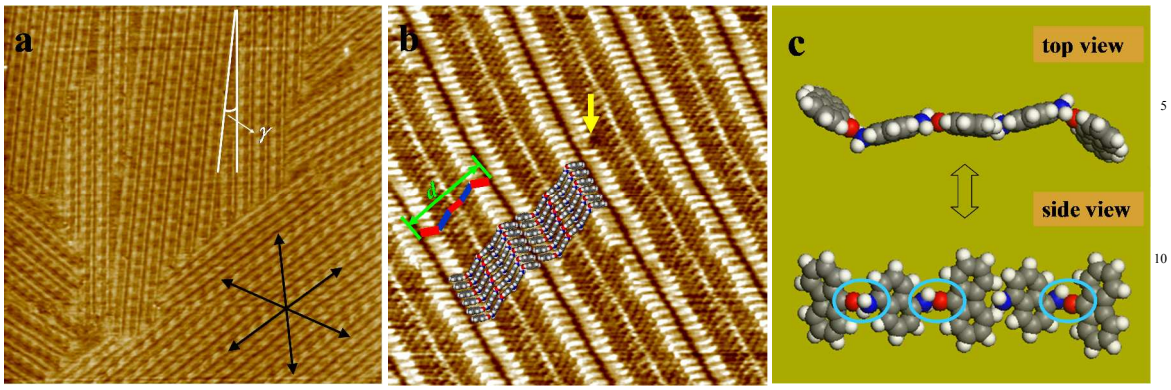

The 2D assembly of co-crystal **C3** is investigated at the liquid/

Fig. 4 (a) Large-scale STM image of **C3** self-assembly at the 1-phenyloctane/HOPG interface. Scan area: 200 nm × 200 nm; Tunneling conditions: V_{bias} = 799 mV, I_t = 454 pA. (b) High-resolution STM image with molecular model of **C3**. Scan area: 15 nm × 15 nm; Tunneling conditions: V_{bias} = 821 mV, I_t = 473 pA. (c) Side view and top view models of single repeating unit.

solid interface. When applying a drop of solution in 1-phenyloctane onto the graphite surface, a lamellar phase is spontaneously formed as shown in Fig. 4a. The uniform electron density evenly spreads over the aromatic molecules and gives a uniform contrast in STM. Thus, together with the close packing of molecules on the surface, it is a difficult task to make the identification of single molecules. As we know, the brightness contrast of STM image is caused by both electronic coupling and topographic factors.[34] For co-crystal **C3** without the alkyl chain, the electronic coupling factor plays a more important role in STM image contrast than the topographic factor. The moiré pattern in Fig. 4a mainly originates from different electron densities in different parts of the standing molecule, which result in various electronic coupling with the STM tip. In Fig. 4a, the two kinds of molecules are organized in several well-packed domains with different sizes in the range of a few tens of nanometers. The domain boundaries and lamella direction can be distinguished easily. Each domain is made up of apparently ordered wide stripes. Most of these domains intersect at about 60° or 120° because of the 3-fold symmetry of the graphite substrate. It illustrates the impact of the substrate on the construction of the physical absorbed adlayer. A careful inspection, however, shows that some lamellar axis has a slight rotation to the adjacent domain as the white lines indicated in Fig. 4a. Measurements show the deflexion angle (γ in Fig. 4a) of the neighboring domains is about 7°. This mismatching to the graphite substrate seems to be explained with the additional shift of the molecules in the direction perpendicular to the molecular row's axis.[35]

Details of the edge-on structure within the single domain are analyzed by a high-resolution STM image shown in Fig. 4b. Unlike the excellent orderings of **C1** and **C2**, a defect indicated by a yellow arrow can be seen in **C3** supramolecular organization. Each lamella consists of two columns, forming a double-herringbone pattern. As the wide zigzag shown in Fig. 4b, one repeating unit consists of five molecules, three fluorenone molecules (red rectangles) and two naphthalene-1,5-diamine molecules (dark blue rectangles). Different molecules arrange alternatively in one lamella and the entire unit is center symmetric. The repeating unit has an average width (d) of 3.4 ± 0.1 nm, which agrees approximately with the sum of the width of the five molecules calculated by Materials Studio. The proposed structural model overlaid on Fig. 4b is almost the same as observed. It is known that the distance of π–π stacking is about 0.34 nm in three-dimensional (3D) crystals. [36] In this self-assembled morphology, the distance between two columns is measured to be 0.45 ± 0.05 nm, a little larger than the spacing of π–π interaction. Besides, fluorenone molecules on both sides have higher contrast and larger width than the middle three molecules. On the basis of the above analysis, we can confirm that the middle three π-conjugated molecules arrange completely vertically to the graphite substrate, while the fluorenone unit at each end is slightly tiled from the HOPG surface adopting an edge-on arrangement. The top view and side view models clearly show the edge-on arrangement of the repeating unit (Fig. 4c). Blue ovals in side view model indicate the strong –N-H…O– hydrogen bonds between naphthalene-1,5-diamine and 9-fluorenone. The formation mechanism of the **C3** herringbone pattern can be explained that, individual aggregates form and adsorb onto the substrate, and then aggregates self-assemble into long uniaxial columns. Hence, the 2D nanocolumn is a result of competition between intermolecular hydrogen bonds and π–π interactions. Note that the possibility of tunneling electrons through such an edge-on layer of the lamellar phase often associated with a remarkable conductivity of the fluorene-based bis-Schiff base compounds. The strongly stacked edge-on ordering also indicates an excellent potential for electron and exciton transport applications.

Conclusions

Integrated studies using STM and X-ray crystallography have demonstrated that the single-crystal (**C1**) crystallize in 2D and 3D with striking homology, the polycrystal (**C2**) has polymorph in 2D and the co-crystal (**C3**) appears different packing pattern between 2D and 3D. The 2D supramolecular architectures depend on the middle tethered spacers and intermolecular hydrogen bonds. The **C1** molecules with a shorter chain form a compact grid pattern due to intermolecular hydrogen bonds as well as the special size and shape of individual molecules. With the increase of tethered alkyl chain length, the **C2** molecules can form two types of linear structures. One lies flat on the substrate while the other adopts an edge-on arrangement. In co-crystal **C3**, naphthalene-1,5-diamine and 9-fluorenone arrange nearly

vertically to the graphite substrate by the π–π interactions and intermolecular hydrogen bonds. In addition, what makes the 2D self-assemble structures different from the 3D space is the competition of various weak non-covalent interactions at the liquid/HOPG interface. To be sure, the STM results at the 1-phenyloctane/HOPG interface highlight that the different crystal forms have obvious relationship with their 2D assembly patterns. Our work may provide a promising approach for designing and tailoring the assembly of 2D supramolecular architectures on the graphite surface.

Acknowledgements

Financial supports from the National Program on Key Basic Research Project (2012CB932900), the National Natural Science Foundation of China (21103053, 51373055) and the Fundamental Research Funds for the Central Universities (SCUT) are gratefully acknowledged.

Notes and references

College of Materials Science and Engineering
South China University of Technology, Wushan Road, Tianhe District, Guangzhou 510640, P. R. China. Tel: (+86)020-22236708
E-mail: msxrmiao@scut.edu.cn, wldeng@scut.edu.cn

1. C. L. D. Gibb and B. C. Gibb, *J. Supramol. Chem.*, 2001, **1**, 39–52.
2. X. R. Miao, L. Xu, Y. J. Li, Z. M. Li, J. Zhou and W. L. Deng, *Chem. Commun.*, 2010, **46**, 8830–8832.
3. S. L. Tait, *ACS Nano*, 2008, **2**, 617–621.
4. J. P. Rabe and S. Buchholz, *Science*, 1991, **253**, 424–427.
5. M. C. Lensen, S. J. T. van Dingenen, J. A. A. W. Elemans, H. P. Dijkstra, G. P. M. van Klink, G. van Koten, J. W. Gerritsen, S. Speller, R. J. M. Nolte and A. E. Rowan, *Chem. Commun.*, 2004, 762–763.
6. N. Severin, I. M. Sokolov, N. Miyashita, D. G. Kurth and J. P. Rabe, *Macromolecules*, 2007, **40**, 5182–5186.
7. J. Zhang, B. Li, X. F. Cui, B. Wang, J. L. Yang and J. G. Hou, *J. Am. Chem. Soc.*, 2009, **131**, 5885–5890.
8. I. Bestel, N. Campins, A. Marchenko, D. Fichou, M. W. Grinstaff and P. Barthelemy, *J. Colloid Interface Sci.,* 2008, **323**, 435–440.
9. G. Fernández, M. Stolte, V. Stepanenko and F. Würthner, *Chem. –Eur. J.*, 2013, **19**, 206–217.
10. C. Cai, L. Wang and J. Lin, *Chem. Commun.*, 2011, **47**, 11189–11203.
11. A. Cristadoro, G. Lieser, H. J. Rader and K. Mullen, *ChemPhysChem*, 2007, **8**, 586–591.
12. A. Cristadoro, M. Ai, H. J. Rader, J. P. Rabe and K. Mullen, *J. Phys. Chem. C*, 2008, **112**, 5563–5566.
13. Y. T. Shen, K. Deng, M. Li, X. M. Zhang, G. Zhou, K. Muellen, Q. D. Zeng and C. Wang, *CrystEngComm*, 2013, **15**, 5526–5531.
14. L. R. Xu, L. Yang and S. B. Lei, *Nanoscale*, 2012, **4**, 4399–4415.
15. D. Rajwar, X. Sun, S. J. Cho, A. C. Grimsdale and D. Fichou, *CrystEngComm*, 2012, **14**, 5182–5187.
16. L. Picard, F. d. r. Lincker, Y. Kervella, M. Zagorska, R. m. DeBettignies, A. Peigney, E. Flahaut, G. Louarn, S. Lefrant, R. Demadrille and A. Pron, *J. Phys. Chem. C*, 2009, **113**, 17347–17354.
17. F. Lincker, N. Delbosc, S. Bailly, R. De Bettignies, M. Billon, A. Pron and R. Demadrille, *Adv. Funct. Mater.*, 2008, **18**, 3444–3453.
18. M. Józefowicz, J. R. Heldt and J. Heldt, *Chem. Phys.*, 2006, **323**, 617–621.
19. F. Jaramillo-Isaza and M. L. Turner, *J. Mater. Chem.*, 2006, **16**, 83–89.
20. X. J. Wang, E. Perzon, J. L. Delgado, P. de la Cruz, F. L. Zhang, F. Langa, M. Andersson and O. Inganas, *Appl. Phys. Lett.*, 2004, **85**, 5081–5083.
21. M. Linares, L. Scifo, R. Demadrille, P. Brocorens, D. Beljonne, R. Lazzaroni and B. Grevin, *J. Phys. Chem. C*, 2008, **112**, 6850–6859.
22. Z. Li, X. Miao, H. Xin and W. Deng, *Mater. Chem. Phys.*, 2010, **124**, 1105–1112.
23. K. K. Ding and C. P. Pan, *Crystallogr. Rep.*, 2013, **58**, 604–607.
24. A. L. Kanibolotsky, R. Berridge, P. J. Skabara, I. F. Perepichka, D. D. C. Bradley and M. Koeberg, *J. Am. Chem. Soc.*, 2004, **126**, 13695–13702.
25. E. J. W. List, R. Guentner, P. S. de Freitas and U. Scherf, *Adv. Mater.*, 2002, **14**, 374–378.
26. L. Romaner, T. Piok, C. Gadermaier, R. Guentner, P. S. de Freitas, U. Scherf, G. Cerullo, G. Lanzani and E. J. W. List, *Synth. Met.*, 2003, **139**, 851-854.
27. L. Xu, X. R. Miao, B. Zha and W. L. Deng, *Chem. – Asia. J.*, 2013, **8**, 926–933.
28. B. Adhikari, A. J. Lough, B. Barker, A. Shah, C. Xiang and H.-B. Kraatz, *Organometallics*, 2014, 10.1021/om500032p.
29. X. Y. Wang, T. F. Jiao, Z. X. Zhang, T. Chen, M. H. Liu, L. J. Wan and D. Wang, *J. Phys. Chem. C*, 2013, **117**, 16392–16396.
30. M. Treier, P. Ruffieux, P. Groning, S. Xiao, C. Nuckolls and R. Fasel, *Chem. Commun.*, 2008, **38**, 4555–4557.
31. C. G. Claessens and J. F. Stoddart, *J. Phys. Org. Chem.*, 1997, **10**, 254–272.
32. W. B. Jennings, B. A. Farrell and J. F. Malone, *J. Org. Chem.*, 2006, **71**, 2277–2282.
33. J. Saiz-Poseu, I. Alcon, R. Alibes, F. Busque, J. Faraudo and D. Ruiz-Molina, *CrystEngComm*, 2012, **14**, 264–271.
34. M. Zhao, P. Jiang, K. Deng, S. S. Xie, G. L. Ge and C. Jiang, *Nanotechnology*, 2009, **20**, 425301.
35. J. Zapala, M. Knor, T. Jaroch, A. Maranda-Niedbala, E. Kurach, K. Kotwica, R. Nowakowski, D. Djurado, J. Pecaut, M. Zagorska and A. Pron, *Langmuir*, 2013, **29**, 14503–14511.
36. T. Sakano, J.-y. Hasegawa, K. Higashiguchi and K. Matsuda, *Chem. – Asia. J.*, 2012, **7**, 394–399.

The observation of two polymorphs indicates C2 can not form single crystal because of the increase of molecular flexibility.